JOURNAL OF COMPUTATIONAL PHYSICS **134,** 253–260 (1997)
ARTICLE NO. CP975691

A Novel Exponentially Fitted Triangular Finite Element Method for an Advection–Diffusion Problem with Boundary Layers

Song Wang

School of Mathematics & Statistics, Curtin University of Technology, GPO Box U1987, Perth 6001, Australia
E-mail: swang@cs.curtin.edu.au

Received August 13, 1996; revised March 10, 1997

In this paper we develop an exponentially fitted finite element method for a singularly perturbed advection–diffusion problem with a singular perturbation parameter ε. This finite element method is based on a set of novel piecewise exponential basis functions constructed on unstructured triangular meshes. The basis functions can not be expressed explicitly, but the values of each of them and its associated flux at a point are determined by a set of two-point boundary value problems which can be solved exactly. A method for evaluating elements of the stiffness matrix is also proposed for the case that ε is small. Numerical results, presented to validate the method, show that the method is stable for a large range of ε. It is also shown by the numerical results that the rate of convergence of the method in an energy norm is of order $h^{1/2}$ when ε is small.

1. INTRODUCTION

This paper deals with the numerical solution of a singularly perturbed advection–diffusion problem with a positive singular perturbation parameter ε by a finite element method. The problem considered here can be regarded as a linear model for the incompressible Navier–Stokes momentum equations. It is well known that solutions to this kind of problem display sharp boundary layers when $\varepsilon \ll 1$ so that classic numerical methods often yield erroneous approximate solutions with spurious oscillations. To overcome this difficulty upwind schemes are often used. However this kind of method may give inaccurate results, especially when ε has the same magnitude as that of the mesh parameter h used (cf., for example, [2, 4]). An alternative way to solve this problem is to use exponentially fitted methods (based on the idea by Alan and Southwell [1]). One example is the exponentially fitted finite volume/element method proposed in [5] and analyzed in [4] which is stable and has an accuracy of $h^{1/2}$ order with respect to a discrete, ε-independent energy norm. An excellent overview of these methods can be found in [8]. To our best knowledge, most of the existing exponentially fitted methods for singularly perturbed advection–diffusion equations in higher dimensions are essentially based on a one-dimensional constant approximation to the flux along element edges (cf., for example, [4]), or a tensor product of the one dimensional approximations along element edges parallel to coordinate axes (cf., for example, [6]). The construction of genuine piecewise exponential basis functions on triangular meshes has been sought, but still remains an open problem except for some special cases (cf., for example [7]). Another progress on this is the divergence free shape functions for the semiconductor device equations proposed recently by Sacco, Gatti, and Gotusso (cf. [9]).

In this paper we present an exponentially fitted Galerkin finite element method based on a novel set of piecewise exponential basis functions constructed on an unstructured triangular mesh. At each point x in a solution domain, the finite element subspace spanned by these basis functions yields constant approximations to the flux projections onto the directions from x to the vertices of the triangle containing x, respectively. These basis functions do not have explicit analytical representations, but the point values of a basis function and its associated flux are determined by a set of two-point boundary value problems which can be solved exactly. Furthermore, each of the basis functions has the same support as that of the corresponding conventional piecewise linear one, and the former contains the latter as a special case (that the coefficient of the advection term is zero). The rest of our paper is organized as follows.

The continuous problem and some preliminaries are described in the next section. In Section 3 we construct the finite element space by deriving a set of the piecewise exponential basis functions. We also present a technique for the evaluation of the entries in the stiffness matrix for the case that ε is small. Numerical results are given in Section 4. The numerical results show that the method is numerically stable for a large range of ε and the rate of convergence of the method in the energy norm is of $h^{1/2}$ order when $\varepsilon \ll 1$.

2. THE PROBLEM

Consider stationary, linear, advection–diffusion problems of the form

0021-9991/97 $25.00

$$-\nabla \cdot (\varepsilon \nabla u - \boldsymbol{a}u) + Gu = F \quad \text{in } \Omega, \tag{2.1}$$

$$u|_{\partial\Omega} = u_D, \tag{2.2}$$

where $\Omega \in \mathbb{R}^2$, $\partial\Omega$ is the boundary of Ω, and ε is a positive parameter. This problem arises from many physical models such as the the decoupled and linearized incompressible Navier–Stokes momentum equations. In this case ε represents 1/Re, where Re denotes the Reynolds number. Without loss of generality, we assume that $u_D = 0$. The case of non-homogeneous boundary condition can be transformed into the homogeneous one by subtracting a known function satisfying the boundary conditions. For simplicity we also assume that $\partial\Omega$ is polygonal. The flux $\boldsymbol{f}$ is defined as

$$\boldsymbol{f} = \varepsilon \nabla u - \boldsymbol{a}u.$$

In what follows $L^2(\Omega)$ denotes the space of square integrable functions with norm $\|\cdot\|_0$ and $H^1(\Omega)$ the usual Sobolev space with norm $\|\cdot\|_1$. The inner product on $L^2(\Omega)$ or on $\boldsymbol{L}^2(\Omega) := (L^2(\Omega))^2$ is denoted by $(\cdot, \cdot)$. We put $H_0^1(\Omega) = \{v \in H^1(\Omega) : v|_{\partial\Omega} = 0\}$. The set of functions which, together with their first partial derivatives, are continuous on $\overline{\Omega}$ is denoted by $C^1(\overline{\Omega})$.

For the coefficient functions we assume that $\boldsymbol{a} \in C^1(\overline{\Omega})$ and that $G, F \in L^2(\Omega)$. We also assume that $\boldsymbol{a}$ and G satisfy

$$\tfrac{1}{2}\nabla \cdot \boldsymbol{a} + G \geq 0 \quad \text{in } \Omega. \tag{2.3}$$

The variational problem corresponding to (2.1) and (2.2) is

PROBLEM 2.1. Find $u \in H_0^1(\Omega)$ such that for all $v \in H_0^1(\Omega)$

$$A(u, v) = (F, v), \tag{2.4}$$

where $A(\cdot, \cdot)$ is a bilinear form on $(H_0^1(\Omega))^2$ defined by

$$A(u, v) = (\varepsilon \nabla u - \boldsymbol{a}u, \nabla v) + (Gu, v). \tag{2.5}$$

Let $\|\cdot\|_E$ be a functional on $H_0^1(\Omega)$ defined by $\|v\|_E^2 = \varepsilon(\nabla v, \nabla v)$. Then, by the well-known Poincaré–Fridriches inequality $\|v\|_E$ is an energy norm on $H_0^1(\Omega)$. Under the condition (2.3) it is possible to show that (cf., for example, [4])

$$A(u, u) \geq \|u\|_E^2 \quad \forall u \in H_0^1(\Omega). \tag{2.6}$$

This implies that $A(\cdot, \cdot)$ is coercive on $H_0^1(\Omega)$ and, thus, by the Lax–Milgram lemma, Problem 2.1 has a unique solution in $H_0^1(\Omega)$.

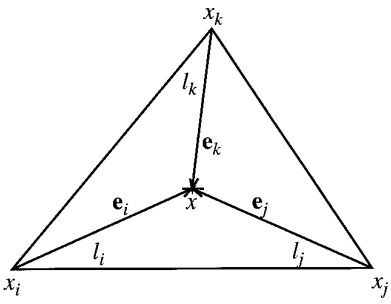

FIG. 3.1. Notation associated with the triangle t.

3. THE FINITE ELEMENT METHOD

In this section we propose a novel conforming finite element for Problem 2.1.

Let T_h be a partition of Ω consisting of triangles having diameters less than or equal to h. The set of vertices of T_h not on $\partial\Omega$ is denoted $\{x_i\}_1^N$.

Corresponding to the mesh T_h, we now construct a space $S_h \subset H_0^1(\Omega)$ of dimension N using the basis functions $\{\phi_i\}_1^N$ defined below. These basis functions are motivated by the idea proposed by Sever [10] and a simpler case that $\boldsymbol{a}$ is irrotational and piecewise constant is discussed in [11].

Let $t \in T_h$ be a triangle with vertices x_i, x_j, and x_k. For any point $x \in t$ we use l_m ($m = i, j, k$) to denote the segment connecting x_m and x, and use $\boldsymbol{e}_m := (e_{m,1}, e_{m,2})$ ($m = i, j, k$) to denote the unit vector from x_m to x (cf. Fig. 3.1). We now find $\phi_i(x)$ and its associated flux $\boldsymbol{f}_i(x) := (f_{i,1}(x), f_{i,2}(x))$ satisfying

$$\frac{d}{d\boldsymbol{e}_m}(\boldsymbol{f}_i \cdot \boldsymbol{e}_m) = \frac{d}{d\boldsymbol{e}_m}\left(\varepsilon \frac{d\phi_i(z)}{d\boldsymbol{e}_m} - a_m \phi_i(z)\right) = 0 \quad \forall z \in l_m, \tag{3.1}$$

and the boundary conditions

$$\phi_i(x_m) = \delta_{im}, \quad \phi_i(x),$$

where $a_m = \boldsymbol{a}(x) \cdot \boldsymbol{e}_m$, δ_{im} denotes the Kronecker delta and $\phi_i(x)$ is yet to be determined. For each x, the above two point boundary value problem yields constant approximations to the flux $\boldsymbol{f}$ along the segments l_m ($m = 1, 2, 3$) (i.e., $\boldsymbol{f}_i \cdot \boldsymbol{e}_m$ is constant on l_m). Since, in (3.1), a_m is independent of z, we can solve (3.1) analytically to obtain

$$\phi_i(z) = \begin{cases} -C_1/a_m + C_2 e^{a_m|z-x_i|/\varepsilon}, & a_m \neq 0 \\ C_1|z - x_i| + C_2, & a_m = 0 \end{cases} \qquad \forall z \in l_m, m = i, j, k,$$

where C_1 ($=\boldsymbol{f}_i \cdot \boldsymbol{e}_m$) and C_2 are two constants to be determined and $|\cdot|$ denotes the Euclidean length. Using the boundary conditions (3.2) we get, for $m = i, j, k$,

$$f_{i,1}e_{m,1} + f_{i,2}e_{m,2} = \boldsymbol{f}_i \cdot \boldsymbol{e}_m = C_1$$
$$= \frac{\varepsilon}{|l_m|}\left[B\left(\frac{a_m|l_m|}{\varepsilon}\right)\phi_i(x) - B\left(-\frac{a_m|l_m|}{\varepsilon}\right)\delta_{im}\right], \quad (3.3)$$

where $B(z)$ denotes the Bernoulli function defined by

$$B(z) = \begin{cases} \dfrac{z}{e^z - 1}, & z \neq 0, \\ 1, & z = 0. \end{cases} \quad (3.4)$$

Now (3.3) defines three linear algebraic equations for the three unknowns $\phi_i(x)$, $f_{i,1}(x)$, and $f_{i,2}(x)$. These three equations can be written as follows:

PROBLEM 3.1. Find ϕ_i and $\boldsymbol{f}_i = (f_{i,1}, f_{i,2})$ such that for any $x \in \bar{t}$

$$D(x)\begin{pmatrix} f_{i,1} \\ f_{i,2} \\ \phi_i \end{pmatrix} = \begin{pmatrix} -\varepsilon B(-a_i|l_i|/\varepsilon) \\ 0 \\ 0 \end{pmatrix}, \quad (3.5)$$

where $D(x)$ is a 3×3 matrix defined by

$$D(x) = \begin{pmatrix} |l_i|e_{i,1} & |l_i|e_{i,2} & -\varepsilon B(a_i|l_i|/\varepsilon) \\ |l_j|e_{j,1} & |l_j|e_{j,2} & -\varepsilon B(a_j|l_j|/\varepsilon) \\ |l_k|e_{k,1} & |l_k|e_{k,2} & -\varepsilon B(a_k|l_k|/\varepsilon) \end{pmatrix}. \quad (3.6)$$

Any solution to Problem 3.1 defines the point values of the function ϕ_i and its associated flux $\boldsymbol{f}_i$ at $x \in \bar{t}$. Similarly we can define functions ϕ_j and ϕ_k associated with x_j and x_k, respectively. The following theorem shows that Problem 3.1 is uniquely solvable for all $x \in \bar{t}$, and that ϕ_i, ϕ_j, and ϕ_k form a system of local basis functions on t.

THEOREM 3.1. *Let $t \in T_h$. Then, for any $x \in \bar{t}$, there exists a unique solution to Problem 3.1. Furthermore, we have*

$$\phi_i(x_i) = 1, \quad \phi_i = 0 \quad \forall x \in \overline{x_j x_k}, \quad (3.7)$$
$$\phi_i + \phi_i + \phi_k = 1, \quad \boldsymbol{f}_i + \boldsymbol{f}_j + \boldsymbol{f}_k = -\boldsymbol{a} \quad \forall x \in \bar{t}, \quad (3.8)$$

where $\overline{x_j x_k}$ denotes the edge of t connecting x_j and x_k.

Proof. To prove that Problem 3.1 is uniquely solvable we need only to show that for any $x \in \bar{t}$ the system matrix $D(x)$ is nonsingular, or $\det D(x) \neq 0$. Let $\sigma_m = a_m|l_m|/\varepsilon$ ($m = i, j, k$). From (3.6) we have, by direct computation,

$$\begin{aligned} \det D(x) = \varepsilon[&|l_i|\,|l_j|B(\sigma_k)(e_{j,1}e_{i,2} - e_{j,2}e_{i,1}) \\ &+ |l_j|\,|l_k|B(\sigma_i)(e_{k,1}e_{j,2} - e_{k,2}e_{j,1}) \\ &+ |l_k|\,|l_i|B(\sigma_j)(e_{i,1}e_{k,2} - e_{i,2}e_{k,1})] \\ = -\varepsilon[&|l_i|\,|l_j|B(\sigma_k)\boldsymbol{e}_z \cdot (\boldsymbol{e}_i \times \boldsymbol{e}_j) \\ &+ |l_j|\,|l_k|B(\sigma_i)\boldsymbol{e}_z \cdot (\boldsymbol{e}_j \times \boldsymbol{e}_k) \\ &+ |l_k|\,|l_i|B(\sigma_j)\boldsymbol{e}_z \cdot (\boldsymbol{e}_k \times \boldsymbol{e}_i) \end{aligned}$$

with $\boldsymbol{e}_z = (0, 0, 1)$ the unit vector perpendicular to t. From the orientations of $\boldsymbol{e}_i$, $\boldsymbol{e}_j$, $\boldsymbol{e}_k$, and $\boldsymbol{e}_z$ (cf. Fig. 3.1) we see that $\boldsymbol{e}_z \cdot (\boldsymbol{e}_i \times \boldsymbol{e}_j)$, $\boldsymbol{e}_z \cdot (\boldsymbol{e}_j \times \boldsymbol{e}_k)$ and $\boldsymbol{e}_z \cdot (\boldsymbol{e}_k \times \boldsymbol{e}_i)$ are all nonnegative, and at least two of them are positive. Furthermore, since $B(\cdot)$ is always positive and at least two of $|l_i|$, $|l_j|$ and $|l_k|$ are positive, we have $\det D(x) \neq 0$.

We now prove (3.7). When $x = x_i$ we have $|l_i| = 0$, and thus from the first equation in (3.5) we obtain $\phi_i(x_i) = 1$. To prove the second part of (3.7), we note that $\boldsymbol{e}_j = -\boldsymbol{e}_k$ if $x \in \overline{x_j x_k}$. Thus we have

$$\begin{vmatrix} |l_i|e_{i,1} & |l_i|e_{i,2} & -\varepsilon B(-a_i|l_i|/\varepsilon) \\ |l_j|e_{j,1} & |l_j|e_{j,2} & 0 \\ |l_k|e_{k,1} & |l_k|e_{k,2} & 0 \end{vmatrix}$$
$$= -\varepsilon B(-a_i|l_i|/\varepsilon)|l_j|\,|l_k|\begin{vmatrix} e_{j,1} & e_{j,2} \\ e_{k,1} & e_{k,2} \end{vmatrix} = 0,$$

since $\boldsymbol{e}_j$ is parallel to $\boldsymbol{e}_k$. So, applying the Cramer's rule to (3.5) and using the above we have $\phi_i = 0$ for all $x \in \overline{x_j x_k}$.

Now we prove (3.8). Let $\phi = \phi_i + \phi_j + \phi_k$ and $(f_1, f_2) = \boldsymbol{f} = \boldsymbol{f}_i + \boldsymbol{f}_j + \boldsymbol{f}_k$. We know that $(f_{i,1}, f_{i,2}, \phi_i)$ satisfies (3.5). Analogously, $(f_{j,1}, f_{j,2}, \phi_j)$ and $(f_{k,1}, f_{k,2}, \phi_k)$ also satisfy (3.5) with the right-hand side vector replaced by $(0, -\varepsilon B(-\sigma_j), 0)^{\mathrm{T}}$ and $(0, 0, -\varepsilon B(-\sigma_k))^{\mathrm{T}}$, respectively. Summing the three linear systems we obtain

$$D(x)\begin{pmatrix} f_1 \\ f_2 \\ \phi \end{pmatrix} = \begin{pmatrix} -\varepsilon B(-\sigma_i) \\ -\varepsilon B(-\sigma_j) \\ -\varepsilon B(-\sigma_k) \end{pmatrix}$$

with $D(x)$ the matrix defined in (3.6). We now verify that $\phi = 1$ and $\boldsymbol{f} = -\boldsymbol{a}$ satisfy the above linear system. From (3.4) it is easy to verify that $B(-z) = e^z B(z)$. Thus, substituting $\phi = 1$ and $\boldsymbol{f} = -\boldsymbol{a}$ into the left-hand side of the above linear system we have, for $m = i, j, k$,

$$
\begin{aligned}
|l_m|\, \boldsymbol{e}_m \cdot (-\boldsymbol{a}) - \varepsilon B(\sigma_m) &= -|l_m| a_m - \varepsilon \frac{|l_m| a_m/\varepsilon}{e^{\sigma_m} - 1} \\
&= -\frac{e^{\sigma_m} |l_m| a_m}{e^{\sigma_m} - 1} \\
&= -\varepsilon e^{\sigma_m} B(\sigma_m) \\
&= -\varepsilon B(-\sigma_m).
\end{aligned}
$$

Thus we have proved (3.8). ∎

For each triangle having x_i as a vertex, where $x_i \notin \partial\Omega$, we have defined a local function ϕ_i and its associated flux $\boldsymbol{f}_i$ as above. These functions do not have explicit representations, but their values at each point are determined uniquely by the linear system (3.5). Combining all the local functions associated with x_i we obtain a hat function ϕ_i defined on the union of all the triangles sharing x_i, denoted by Ω_i. From Theorem 3.1. we see that this ϕ_i is unity at x_i and 0 on $\partial\Omega_i$. This hat function ϕ_i can then be extended to $\overline{\Omega}$ by defining $\phi_i(x) = 0$ for all $x \in \Omega \backslash \overline{\Omega}_i$. Applying Cramer's rule to (3.5) we see that in each triangle t, ϕ_i, can be expressed as a ratio of a function of a_m and $|l_m|$ $(m = i, j, k)$ and the determinant $\det(D)$. Since both the numerator and the denominator in the expression for ϕ_i contain only polynomials and exponentials of a_m and $|l_m|$ $(m = i, j, k)$, ϕ_i is differentiable in t, because $\boldsymbol{a} \in C^1(\overline{\Omega})$. This implies that $\phi_i \in H^1(t)$. (In fact, $\phi_i \in H^1(t)$ if $\boldsymbol{a} \in (H^1(t))^2$.) If we can show that ϕ_i is continuous across inter-element boundaries in Ω_i, then $\phi_i \in C^0(\overline{\Omega}) \cap H_0^1(\Omega)$. Let t_1 and t_2 be the two triangles sharing the edge $\overline{x_i x_j}$, and let $\phi_{i,1}$ and $\phi_{i,2}$ are the local functions on t_1 and t_2 respectively defined by (3.5). When $x \in \overline{x_i x_j}$ we have that $(e_{j,1}, e_{j,2}) = -(e_{i,1}, e_{i,2})$ (cf. Fig. 3.1). Thus multiplying the first equation in (3.5) by $|l_j|$ and the second equation by $|l_i|$, and adding the resulting equations up we have

$$
-[|l_j| B(\sigma_i) + |l_i| B(\sigma_j)] \phi_{i,m} = -|l_j| B(-\sigma_i), \quad m = 1, 2, \quad (3.9)
$$

where $\sigma_n = a_n l_n/\varepsilon$ $(n = i, j)$. So both $\phi_{i,1}$ and $\phi_{i,2}$ on $\overline{x_i x_j}$ are determined by the above equation, and thus ϕ_i is continuous across $\overline{x_i x_j}$ because $\boldsymbol{a}$ is continuous on $\overline{\Omega}$ and $B(z)$ is a continuous function.

We remark that when $\boldsymbol{a} \equiv 0$, the basis function ϕ_i reduces to the standard piecewise linear basis function. Obviously ϕ_i is a hat function on its support Ω_i. To visualize ϕ_i in a typical case, we choose Ω_i to be the unit square $[0, 1] \times [0, 1]$ consisting of four triangles formed by the four sides and the two diagonals of the square. We then solve (3.5) with $\boldsymbol{a} = (x + y, y)$ on each triangle. The results for $\varepsilon = 0.5$ and 0.1 are plotted in Fig. 3.2. From these plots we see that $\phi_i = 1$ at the center and zero on the boundary of Ω_i, as proved in Theorem 3.1. It is also seen that the hat functions are continuous on Ω_i.

We now put $S_h = \text{span}\{\phi_i\}_1^N$. From the above discussion we see $S_h \subset C^0(\overline{\Omega}) \cap H_0^1(\Omega)$. Using this finite element space S_h we define the following Bubnov–Galerkin problem.

PROBLEM 3.2. Find $u_h \in S_h$ such that for all $v \in S_h$

$$
A(u_h, v_h) = (F, v_h) \quad (3.10)
$$

with $A(\cdot, \cdot)$ the bilinear form on $(H_0^1(\Omega))^2$ defined by (2.5).

Because $S_h \subset H_0^1(\Omega)$, from (2.6) we have

$$
A(v_h, v_h) \geq \|v_h\|_E^2 \quad \forall v_h \in S_h;
$$

i.e., $A(\cdot, \cdot)$ is coercive on $S_h \times S_h$. Therefore, there exists a unique solution to Problem 3.2.

The stability and convergence of the method involve intensive mathematical analysis and are currently under development. In the present paper we concentrate on the computation of the method. The numerical results in the next section show that the method is numerically stable when $\varepsilon \ll h$ and converges, in the energy norm, to the exact solution at the rate of $h^{1/2}$ order.

Let $u_h = \sum_{j=1}^N u_j \phi_j$ and $v_h = \phi_i$ $(i = 1, 2, ..., N)$. Substituting these into (3.10) we obtain a linear algebraic system of the form

$$
B\boldsymbol{u} = \boldsymbol{b},
$$

where $\boldsymbol{u} = (u_1, u_2, ..., u_N)^{\mathrm{T}}$, $\boldsymbol{b}$ is a known vector, and $B := (b_{ij})_{N \times N}$ is an $N \times N$ unsymmetric matrix with

$$
b_{ij} = \int_\Omega (\varepsilon \nabla \phi_j - \boldsymbol{a} \phi_j) \cdot \nabla \phi_i \, dx = \int_\Omega \boldsymbol{f}_j \cdot \nabla \phi_i \, dx. \quad (3.11)
$$

We comment that $\nabla \phi_i$ is not given explicitly in (3.5), but it can be obtained from

$$
\nabla \phi_i = ((f_{i,1} + a_i \phi_i)/\varepsilon, (f_{i,2} + a_i \phi_i)/\varepsilon),
$$

where $(f_{i,1}\ f_{i,2}\ \phi_i)$ is the solution to (3.5). When ε is small, $\nabla \phi_i$ is peaked along one side of a triangle, which makes the numerical evaluation of (3.11) difficult. To overcome this difficulty, we observe that the variation of $\boldsymbol{f}_i$ in any element t is much smaller than that of $\nabla \phi_i$. So we may approximate b_{ij} by

$$
b_{ij} \approx \sum_{t \in T_h} \boldsymbol{f}_j(b_t) \cdot \int_t \nabla \phi_i \, dx,
$$

where b_t denotes the barycenter of the element t. This is equivalent to applying the one-point quadrature rule to the term $\boldsymbol{f}_i$. Now, integration by parts we get

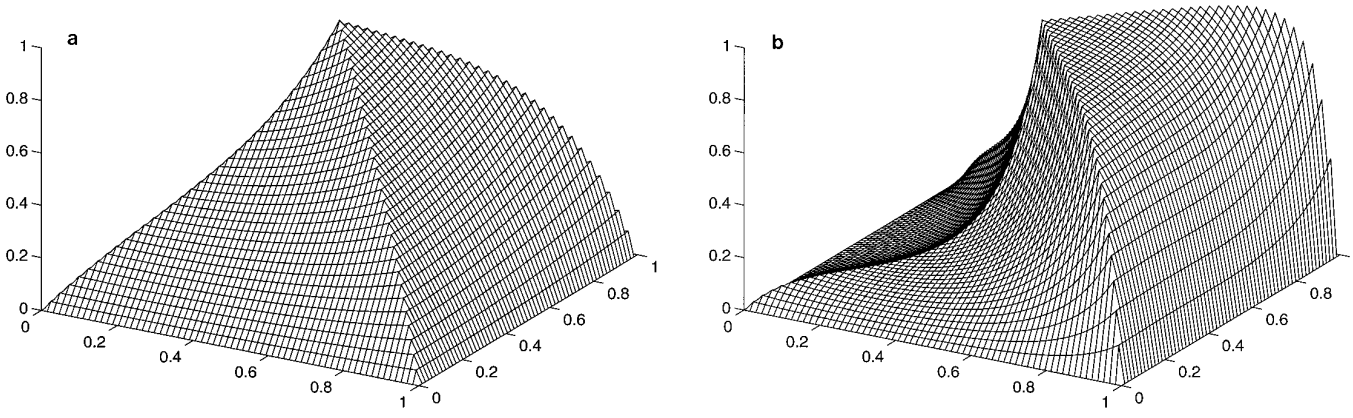

FIG. 3.2. Hat functions: (a) $\varepsilon = 0.5$; (b) $\varepsilon = 0.1$.

$$b_{ij} \approx \sum_{t \in T_h} \boldsymbol{f}_j(b_t) \cdot \int_{\partial t} \boldsymbol{n} \phi_i \, ds. \tag{3.12}$$

Here ∂t denotes the boundary of t and $\boldsymbol{n}$ the unit outward normal vector of ∂t. The line integral in (3.12) is easy to evaluate numerically. This is because along each side of t, ϕ reduces to a one-dimensional exponential hat function determined by (3.9) (cf. Fig. 3.2).

4. NUMERICAL EXPERIMENTS

To validate the method in the previous section, numerical experiments were performed. The implementation of the previous method needs numerical integrations on both segments and triangles. For all the numerical solutions below we use the 2-point Gauss quadrature rule for all the line integrals in the right side of (3.12) and the 9-point quadrature rule for all area integrals on triangles. (The latter can be found, for example, in [3, p. 183].) All computations were carried out in double precision on a UNIX workstation.

The test problem is chosen to be (cf. [5])

$$\begin{aligned} -\nabla \cdot (\varepsilon \nabla u - \boldsymbol{a} u) + 2u &= F \quad \text{in } \Omega = (0,1)^2, \\ u &= 0 \quad \text{on } \partial\Omega, \end{aligned}$$

with $\boldsymbol{a} = (1, 1)$ and the exact solution

$$u = xy(1 - e^{(x-1)/\varepsilon})(1 - e^{(y-1)/\varepsilon}).$$

The right-hand side function is

$$\begin{aligned} F = {} & x(1 - e^{(x-1)/\varepsilon})[1 + e^{(y-1)/\varepsilon} + y(1 - e^{(y-1)/\varepsilon})] \\ & + y(1 - e^{(y-1)/\varepsilon})[1 + e^{(x-1)/\varepsilon} + x(1 - e^{(x-1)/\varepsilon})]. \end{aligned}$$

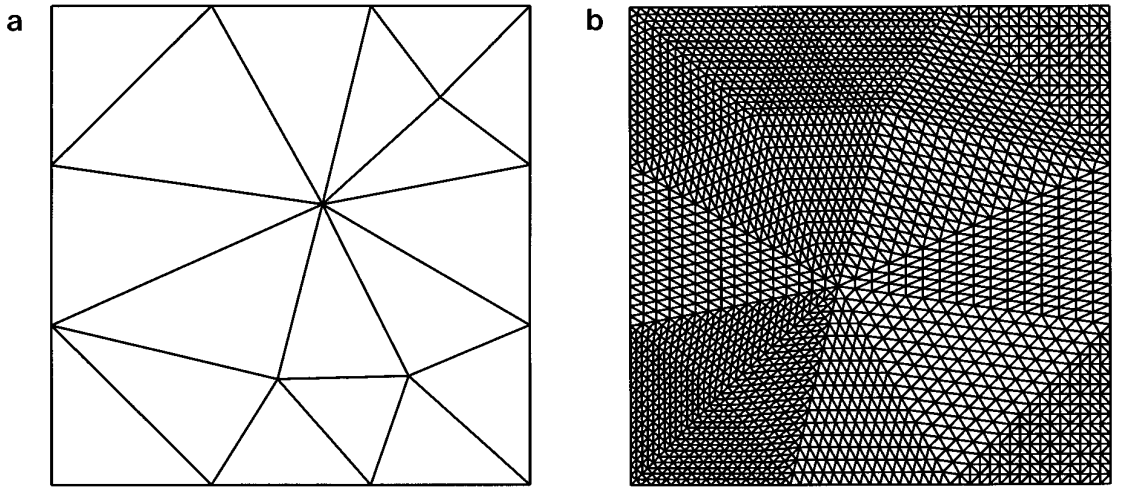

FIG. 4.1. (a) The initial mesh. (b) The refined mesh with 2401 mesh nodes.

TABLE I

Computed Rates of Convergence in Various Norms for Different ε

ε	$\|\cdot\|_E$	$\|\cdot\|_0$	$\|\cdot\|_{\infty,h}$
1	1.00	2.00	1.74
10^{-1}	0.97	1.90	1.84
10^{-2}	0.71	1.15	0.70
10^{-3}	0.55	0.64	−0.17
10^{-4}	0.53	0.65	−0.01
10^{-5}	0.52	0.67	0.23
10^{-6}	0.52	0.68	0.23
10^{-7}	0.52	0.68	0.23

Obviously this problem has two boundary layers along $x = 1$ and $y = 1$.

We first evaluate numerically the rates of convergence of the method in different norms. The domain Ω is first triangulated into 18 triangles with four randomly generated interior nodes. We then smooth the mesh by moving each interior node to the average of its neighboring nodes. The maximum angle and the minimum angles in the resulting mesh are respectively 95.1° and 31.6°, and the mesh parameter $h_1 \approx \frac{1}{3}$. This mesh is then refined repeatedly by adding the midpoints of the edges. Thus we obtain a sequence of meshes corresponding to the mesh parameters $\{h_i\}_1^6$, where $h_k = h_{k-1}/2$ ($k = 2, 3, 4, 5, 6$). The initial mesh and the mesh corresponding to $k = 5$ with 2401 mesh nodes are shown in Fig. 4.1.

For each $k = 1, 2, 3, 4, 5$ we define a rate of convergence p_k by

$$p_k = \log_2 \frac{\|u_{h_k} - u\|_E}{\|u_{h_{k+1}} - u\|_E},$$

where u_{h_k} denotes the numerical solution obtained using the mesh with parameter h_k and $\|\cdot\|_E$ is the energy norm defined in Section 2. Then, we define the computed rate of convergence to be $p = (\sum_{i=1}^{5} p_k)/5$. Based on the above method we also define the computed rates of convergence in the L^2-norm

$$\|u_h - u\|_0 = \left(\int_\Omega |u_h - u|^2 \, dx \right)^{1/2}$$

and in the discrete maximum norm

$$\|u_h - u\|_{\infty,h} = \max_{1 \le i \le N} |u_i - u(x_i)|.$$

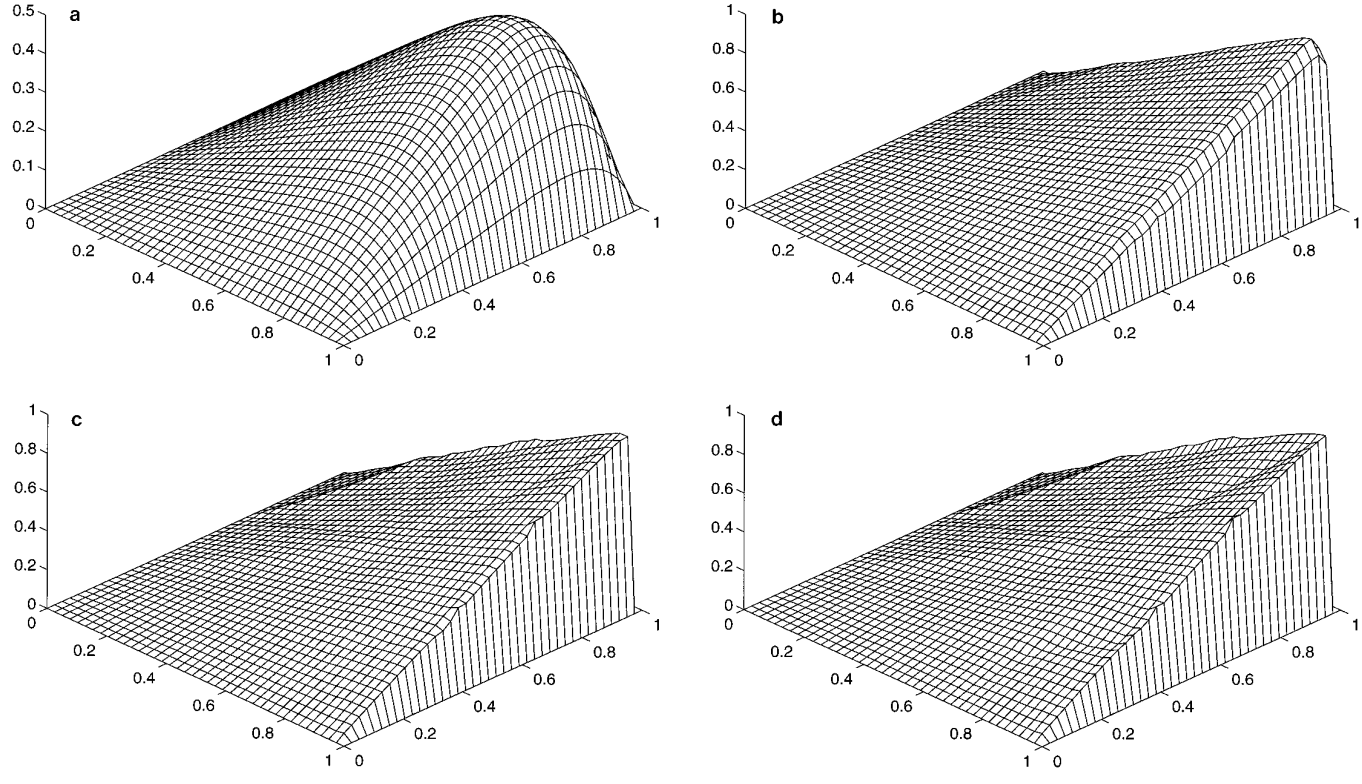

FIG. 4.2. Results for different values of ε: (a) 0.1; (b) 0.01; (c) 0.001; (d) 0.0001.

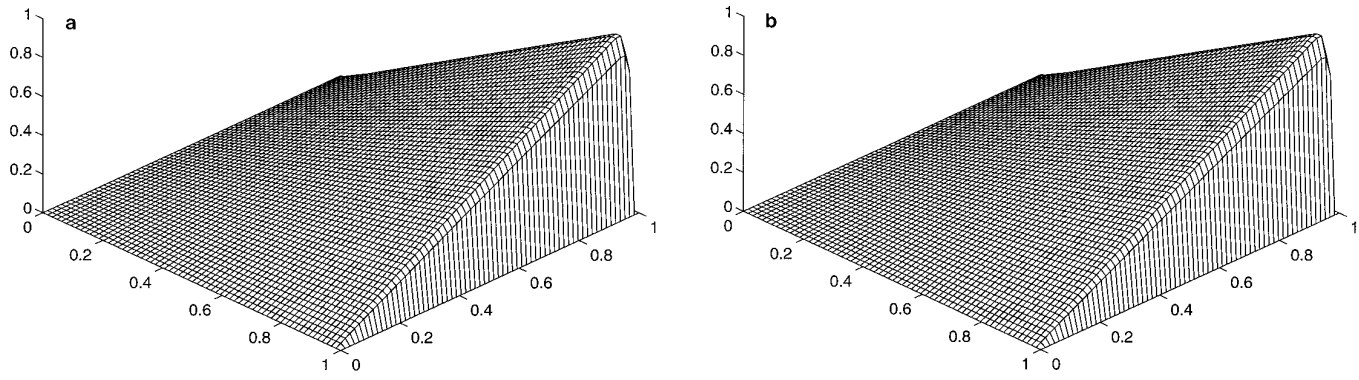

FIG. 4.3. Results obtained using the uniform mesh: (a) $\varepsilon = 0.001$; (b) $\varepsilon = 0.0001$.

The computed values of p for different values of ε are listed in Table I. From the table we see that when ε is small, the computed rates of convergence in $\|\cdot\|_E$ and $\|\cdot\|_0$ are about 0.5 and 0.65, respectively. The former rate is in agreement with the known result for the one-dimensional exponential fitting method and this rate of convergence is optimal (cf., for example, [6]). The computed rate of convergence in the maximum norm $\|\cdot\|_{\infty,h}$ is positive except for $\varepsilon = 10^{-3}$ and 10^{-4}.

To demonstrate the numerical stability of the method, we plot, in Fig. 4.2, the results of the test problem for various ε obtained using the triangular mesh depicted in Fig. 4.1b. Because the mesh is unstructured, we first evaluate the nodal values of the approximate solution at the vertices of the 40×40 uniform grid using the conventional piecewise linear interpolation. Then the interpolated nodal values at the vertices of the uniform grid are plotted. From this figure we see that there are no spurious oscillations in the numerical solutions although these solutions display sharp boundary layers. It is also seen that the results for $\varepsilon < 0.1$ are piecewise smooth. They are not smooth or are less smooth across the element edges of the initial mesh depicted in Fig. 4.1a This is because the refined mesh in Fig. 4.1b changes its mesh density and pattern across the interelement boundaries of the initial mesh. To improve the pointwise accuracy of the approximate solution in regions away from the layers, we may use uniform meshes. Figure 4.3 contains the numerical solutions using the mesh obtained by dividing each square in the 65×65 uniform mesh into two triangles by its diagonal from SE to NW. From this figure we see that the results are much smoother than those in Fig. 4.2. This is probably due to the superconvergence of the method in regions away from the layers when a uniform mesh is used.

5. CONCLUSIONS

In this paper we presented an exponentially fitted finite element method with triangular elements for a singularly perturbed advection–diffusion equation. The method is based on a set of novel piecewise exponential basis functions. The basis functions can not be expressed explicitly, but the point values of each of them and its associated flux are determined by a set of two-point boundary value problems. Numerical experiments were performed to validate the usefulness of the method and the numerical results showed that, when $\varepsilon \ll h$, the method is numerically stable and converges to the exact solution in the energy norm at a rate of $h^{1/2}$.

ACKNOWLEDGMENT

The author is grateful to the referees for several helpful contributions. The support of the Australian Research Council is also gratefully acknowledged.

REFERENCES

1. D. N. de G. Allen and R. V. Southwell, Relaxation methods applied to determine the motion, in two dimensions, of a viscous fluid past a fixed cylinder, *Quart. J. Mech. Appl. Math.* **8,** 129 (1955).
2. A. Brandt and I. Yavneh, Inadequacy of first-order upwind difference schemes for some circulating flows, *J. Comput. Phys.* **93,** 128 (1991).
3. P. G. Ciarlet, *The Finite Element Method for Elliptic Problems* (North-Holland, Amsterdam, 1978).
4. J. J. H. Miller and S. Wang, A new non-conforming Petrov–Galerkin finite element method with triangular elements for a singularity perturbed advection-diffusion problem, *IMA J. Numer. Anal.* **14,** 257 (1994).
5. J. J. H. Miller and S. Wang, An exponentially fitted finite element volume method for the numerical solution of 2D unsteady incompressible flow problems, *J. Comput. Phys.* **115,** No. 1, 56 (1994).
6. E. O'Riordan and M. Stynes, A global uniformly convergent finite element method for a singularly perturbed elliptic problem in two dimensions'' *Math. Comput.,* **57,** 47–62 (1991).
7. E. O'Riordan and M. Stynes, An analysis of some exponentially fitted finite element methods for singularly perturbed elliptic problems, in *Computational Methods for Boundary and Interior Layers in Several Dimensions,* edited by J. J. H. Miller (Boole, Dublin, 1991), p. 138.
8. H.-G. Roos, M. Stynes, and L. Tobiska, *Numerical Methods for Singu-*

larly Perturbed Differential Equations (Springer-Verlag, Berlin/Heidelberg, 1996).

9. R. Sacco, E. Gatti, and L. Gotusso, Divergence free shape functions for a finite element solution of the drift-diffusion equations in semiconductors, *Preprint 140/P,* Dept of Math., Polytechnic of Milan, 1994.
10. M. Sever, Discretization of time-dependent continuity equations, in *Proceedings of the 6th International NASECODE Conference,* edited by J. J. H. Miller, Boole, Dublin, 1988, p. 71.
11. S. Wang, A new exponentially fitted triangular finite element method for the continuity equations in the drift-diffusion model of semiconductor devices. [submitted]